



# Carbon and nutrient dynamics during coastal upwelling off Cape Blanco, Oregon

A. van Geen<sup>a,\*</sup>, R.K. Takesue<sup>a</sup>, J. Goddard<sup>a</sup>, T. Takahashi<sup>a</sup>,  
J.A. Barth<sup>b</sup>, R.L. Smith<sup>b</sup>

<sup>a</sup>*Lamont-Doherty Earth Observatory of Columbia University, Palisades, NY 10964, USA*

<sup>b</sup>*College of Oceanic and Atmospheric Sciences, Oregon State University, Corvallis, Oregon, OR 97331, USA*

Received 31 March 1998; received in revised form 1 December 1998; accepted 25 February 1999

## Abstract

The partial pressure of carbon dioxide ( $\text{PCO}_2$ ) and concentrations of the nutrients phosphate (P) and silicate (Si) in coastal surface waters within a 100 km  $\times$  300 km area centered on Cape Blanco, Oregon, were mapped at high resolution during August 17–27, 1995. Alkalinity and the concentration of total  $\text{CO}_2$  were determined on a subset of stored samples. Over the 9–18°C range in sea-surface temperatures encountered during the cruise,  $\text{PCO}_2$ , and P and Si concentrations varied between 150–690  $\mu\text{atm}$ , < 0.1–1.8, and < 1–33  $\mu\text{mol/kg}$ , respectively. Spatial variations in the intensity of coastal upwelling set the wide range in surface water properties. Acoustic Doppler current profiler data collected throughout the cruise indicate the advective nature of many chemical features.  $\text{PCO}_2$  data also indicate the presence of an intense phytoplankton bloom in continental shelf waters along the coast north of Cape Blanco, with little evidence of biological drawdown to the south. The available data do not provide an unambiguous explanation for this contrast. Surf-zone water was sampled from shore at 17 locations along the cruise areas on August 25 and 26, 1995, concurrently with the shipboard measurements.  $\text{PCO}_2$ , and P and Si concentrations, varied in the range 250–640  $\mu\text{atm}$ , 0.3–2.0, and 1.1–42  $\mu\text{mol/kg}$ , respectively. North of Cape Blanco, the chemical expression of upwelling was considerably stronger in the surf-zone than at all locations sampled on board ship because the phytoplankton bloom did not extend to the coast. South of Cape Blanco, concentrations of upwelling tracers measured on board ship within a distance of 5–10 km from the coast and in the surf-zone were comparable. Vertical nutrient profiles across the continental shelf show that the composition of surf-zone water is consistent with conservative advection of nutrient-enriched bottom water from the edge of the continental shelf to the surf-zone. © 2000 Elsevier Science Ltd. All rights reserved.

\* Corresponding author. Tel.: 1-914-365-8644; fax: 1-914-365-8154.

E-mail address: avangeen@ldeo.columbia.edu (A. van Geen)

## 1. Introduction

According to Sverdrup et al. (1942), Thorade (1909) first explained the presence of cold surface water off the coast of Baja California on the basis of the recent Ekman theory of wind-driven circulation. Hydrographic surveys and time series collected in the California Current during the following decades led to a basic understanding of the relation between coastal upwelling and biological productivity in eastern boundary current systems (e.g. Sverdrup and Allen, 1939). The suite of parameters measured in these pioneering studies typically included temperature, salinity, nutrient concentrations, and plankton counts. Yet, using the same techniques, the role of coastal upwelling in explaining the elevated productivity of the California Current system could still credibly be challenged until fairly recently. On the basis of data collected during the California Cooperative Fisheries Investigation (CalCOFI) program, Chelton et al. (1982) argued that nutrients were supplied to the California Current by advection of nutrient-rich surface water from the north rather than by upwelling along the coast. This hypothesis has not been supported by more recent studies which demonstrate that upwelled water is transported offshore and that low-salinity water advected from the north is typically nutrient-depleted (Huyer et al., 1991; Chavez et al., 1991). New approaches used in these later studies, such as satellite imagery and shipboard acoustic Doppler current profiling, also have demonstrated the high degree of spatial and temporal variability of circulation inshore of the California Current (Kosro et al., 1991).

If surveying the physical features of a coastal upwelling system with sufficient resolution remains a challenge, it is not surprising that the highly patchy biological response to coastal upwelling is only partially understood. Sverdrup and Allen (1939) already noted that while upwelling was needed to cause a diatom bloom, recently upwelled water did not always contain many diatoms. Barber et al. (1971), MacIsaac et al. (1985), and Wilkerson and Dugdale (1987) postulated a form of “preconditioning” of source waters to explain why diatom growth could be delayed by several days following upwelling. Whether adjustment to light, population seeding, generation of detoxifying ligands, or trace metal input could explain such a delay remains an open question. The purpose of this paper is to document pronounced contrasts in the biological response to upwelling off the coast of Oregon from the distribution of chemical properties in surface waters measured at high resolution on board ship.

Our study focuses on the chemical expression of coastal upwelling from, literally, the surf-zone to the edge of the continental shelf. The cruise was designed to observe the separation of a baroclinic coastal jet from the continental shelf near Cape Blanco, Oregon (Barth et al., 2000). Between August 17 and 27, 1995, a 100 km × 300 km area centered on 43°N latitude was intensively studied by towing a conductivity-temperature-depth (CTD) recording instrument aboard the undulating platform SeaSoar, by mapping current velocities with a shipboard acoustic Doppler current profiler (ADCP), by collecting subsurface water with Niskin bottles, and by deploying satellite-tracked drifters (Barth et al., 2000). We present high-resolution measurements of the partial pressure of carbon dioxide (PCO<sub>2</sub>) and concentrations of the nutrients

phosphate (P) and silicate (Si) in surface waters during the cruise, as well as concurrent determinations of these parameters in surf-zone water along the cruise area. The observations are used to address three questions: (1) How does the intensity of upwelling vary across the continental shelf? (2) Where do upwelled waters outcrop and from what depth do they originate? (3) Which features of shelf circulation appear to favor/restrict a biological response to upwelling?

Following a review of the main physical observations by Barth et al. (2000) on the basis of surface temperature and salinity distributions, as well as ADCP data, we examine the main features of the distribution of chemical properties. We document a sharp contrast in the biological response to coastal upwelling with an intense nearshore phytoplankton bloom north of Cape Blanco and little indication of biological activity to the south. We then show that the chemical expression of coastal upwelling is generally stronger in the surf-zone than in coastal surface waters sampled from the ship. On the basis of a vertical section of chemical properties across the continental shelf, we show that the composition of surf-zone water is similar to that of the bottom mixed-layer over the shelf. We propose that this is due to rapid transport of water from this layer to the surf-zone. In the discussion that follows, the relationships between  $\text{PCO}_2$  and total dissolved  $\text{CO}_2$ , surface temperature, alkalinity, and gas exchange are examined in some detail. We conclude by comparing variations in surface physical and chemical properties for two cross-shelf sections, one representative of the high-productivity region north of Cape Blanco, and the other from the low-productivity region south of Cape Blanco.

## 2. Methods

### 2.1. Continuous underway measurements

$\text{PCO}_2$  in the ship's laboratory seawater supply was monitored continuously during the cruise with a "shower-type" flow-through equilibrator modified from Broecker and Takahashi (1966). The residence time of the water in the  $\sim 20$  l equilibrator was  $\sim 1$  min, and the headspace of the equilibrator was sampled every 2 min for  $\text{PCO}_2$  determinations with an infrared gas analyzer (LI-COR, Lincoln, Nebraska). The analyzer was calibrated every 76 min with four gas standards containing 856.5, 555.3, 361.7, and 249.2 ppm mole fraction of  $\text{CO}_2$  in dry air. Atmospheric  $\text{PCO}_2$  at an intake placed on the bow of the ship also was measured every 76 min.  $\text{PCO}_2$  measured in the equilibrator was converted to  $\text{PCO}_2$  at sea-surface temperature (SST) using the temperature recorded in the equilibrator water and in the seawater intake (5 m below the surface) and a temperature coefficient of 4.23%  $\text{PCO}_2$  per  $^\circ\text{C}$  (Takahashi et al., 1993). The correction was commonly less than 0.8% of the measured  $\text{PCO}_2$  value.

Surface concentrations of the nutrients P and Si were measured every 3 min during most of the cruise in a stream of seawater supplied from a device towed over the side of the ship. Nitrate + nitrite concentrations ( $\text{NO}_3^-$ ) were measured on August 17–18 and August 24–27 only because the Cd-reduction column leaked. The towed device consisted of a bathythermograph towed horizontally,  $\sim 1$  m below the surface and

~ 3 m from the side of ship, and a Teflon-lined polyethylene tube (3/8" ID) with one end projecting ~ 2 cm forward of the bathythermograph and the other leading to the shipboard laboratory. The flow of seawater through a peristaltic pump (~ 0.5 l/min, Cole-Parmer) continuously overflowed a ~ 100 ml vessel that was sampled automatically by a Lachat QuikChem 8000 flow-injection analyzer (Milwaukee, WI). The system uses standard colorimetric methods adapted for flow injection analysis following the approach of Johnson and Petty (1983). Low-nutrient water supplied by a shipboard MQ + system (Millipore, MA) was used to make a NaCl carrier solution that matched the refractive index of seawater. Nutrients standards prepared in the same NaCl matrix were analyzed at the beginning and at the end of each run to correct for drift (typically < 10% change in sensitivity over 3 h). The unspiked NaCl solution, assumed to contain negligible nutrient levels, was used as a blank. Detection limits of 0.1, 0.2, and 0.1  $\mu\text{mol/kg}$  calculated for P, Si, and  $\text{NO}_3$ , respectively, are three-fold the typical standard deviation for a NaCl blank solution monitored every 10 samples. The precision was estimated to be on the order of  $\pm 1$ ,  $\pm 1$ , and  $\pm 2\%$  for P, Si, and  $\text{NO}_3$ , respectively, based on standard deviations for 1.5, 40, and 15  $\mu\text{mol/kg}$  standards measured 10 times over the course of a 3-h run.

## 2.2. Discrete shipboard sampling

Water samples for total  $\text{CO}_2$  ( $\text{TCO}_2$ ) determinations were collected in sterilized 500-ml Pyrex glass bottles from the surface water line feeding the  $\text{PCO}_2$  equilibrator. Before storage, 250  $\mu\text{l}$  of a 50%-saturated mercuric chloride solution were added to each bottle to prevent biological alteration of the  $\text{CO}_2$  concentration.  $\text{TCO}_2$  in stored waters was determined by coulometry at Lamont-Doherty (Chipman et al., 1993). The mass of water samples analyzed was determined by weighing a sampling syringe before and after each sample introduction to the stripping column of a coulometer. Reference solutions supplied by A. Dickson (SIO) were analyzed concurrently with the samples, and our results were consistent within  $\pm 1.5 \mu\text{mol/kg}$  with manometric determinations by C.D. Keeling (SIO). Selected 10 l Niskin bottles from the nine rosette casts taken in water depths ranging from 31 to 1650 m also were sampled for  $\text{TCO}_2$  and nutrients. Nutrient samples collected in 60 ml Nalgene bottles cleaned in MQ water were preserved with the addition of 60  $\mu\text{l}$  of 12 N HCl (Seastar, Vancouver, B.C.) and analyzed in port at the end of the cruise with the Lachat system. The relation between P and Si of profile samples for two offshore profiles collected ~ 46 km from the coast was consistent with the underway surface nutrient data collected throughout the cruise area. For reasons we do not understand, P concentrations measured in profile samples over the shelf were systematically higher by ~ 0.2  $\mu\text{mol/kg}$  in the 1.2–2.0  $\mu\text{mol/kg}$  range than P concentrations measured underway in surface waters containing equal Si levels. One possible explanation is the presence of a relatively minor P pool in the water column over the shelf that responds to colorimetry only in acidified samples.

Alkalinity was measured using a new  $\text{PCO}_2$ – $\text{TCO}_2$  method in all discrete water samples collected on board the ship and three samples collected in the surf-zone (Appendix, Tables A1, A3). After a stored water sample bottle was first opened and

used for the  $\text{TCO}_2$  analyses, the remaining water sample (about 400 ml) was kept in the same capped bottle for several days. The sample was analyzed for  $\text{PCO}_2$  at  $20.0^\circ\text{C}$  using a closed volume equilibration method of Chipman et al. (1993), and this was followed immediately by another  $\text{TCO}_2$  determination in the equilibrated water. This pair of  $\text{PCO}_2$  and  $\text{TCO}_2$  values which were measured nearly concurrently was used to compute the total alkalinity by means of the computational scheme for carbonate equilibria described in Peng et al. (1987). The salinity and concentration of P and Si in the sample were used to compute the alkalinity contributions from the dissociation of boric, phosphoric and silicic acids. In six separate samples, these measurements were repeated, and the results of the duplicate measurements are listed in Appendix Tables A2, A3. On the basis of these six pairs of determinations, the precision of the measurements is estimated to be about  $\pm 2 \mu\text{eq/kg}$ . In addition, the alkalinity value obtained for each of the three surf-zone samples was compared with that computed using the field-equilibrated  $\text{PCO}_2$  (see below) and the initial  $\text{TCO}_2$  data obtained from the stored bottle sample. The three pairs of alkalinity values agree within  $\pm 3 \mu\text{eq/kg}$ . Therefore, the alkalinity values measured entirely in the laboratory were consistent with those estimated from a combination of field ( $\text{PCO}_2$ ) data and laboratory ( $\text{TCO}_2$ ) data.

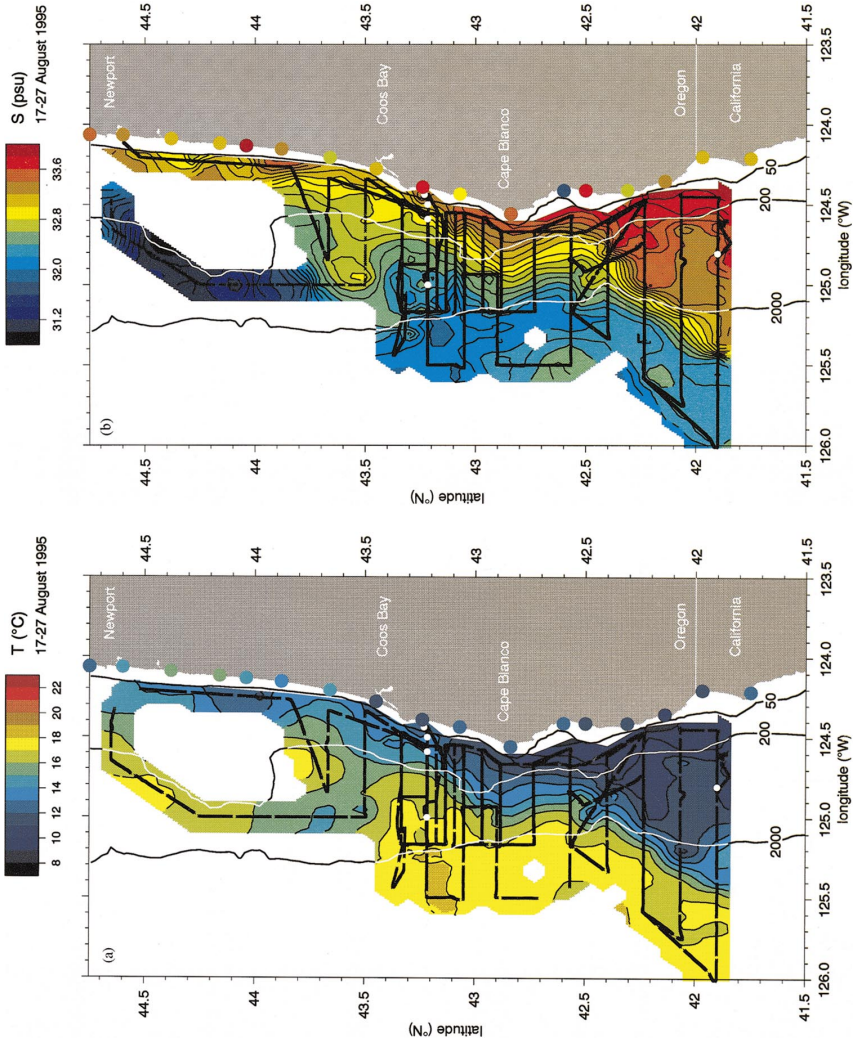
### 2.3. Surf-zone sampling

Towards the end of the cruise on August 25 and 26, surf-zone samples were collected from the beach at 17 sites distributed along the cruise area ( $41.8^\circ\text{N}$  to  $44.6^\circ\text{N}$ ). For  $\text{PCO}_2$  determinations, a portable, closed-volume, gas recirculation system was used on the beach to obtain a gas sample equilibrated with surf-zone water (Takahashi et al., 1991). The 4l glass vessel of this device was equilibrated by recirculation through a gas disperser immersed in the vessel at a rate of 500 ml/min while monitoring temperature and pressure. A different 200 ml glass ampoule was placed in the gas circulation loop for each sample, sealed at the end of a 20 min recirculation period, and shipped back to the laboratory. The  $\text{CO}_2$  content of the equilibrated gas in the ampoule was measured using a gas chromatograph (Chipman et al., 1993) and converted to in situ  $\text{PCO}_2$  based on the recorded surf-zone water temperature and equilibrium pressure. Sterilized 500 ml glass flasks were also filled with surf-zone water and poisoned with  $\text{HgCl}_2$  for  $\text{TCO}_2$  determination in the laboratory.

Salinity and nutrient samples were collected at the end of a 3-m pole following the procedure of van Geen and Husby (1996). Salinity samples were transferred to glass milk-dilution bottles closed with PolySeal caps for determination at Lamont-Doherty using a Guildline salinometer standardized with I.A.P.S.O. water. Nutrient samples were immediately filtered through a  $0.4\text{-}\mu\text{m}$  disposable polyethylene filter, acidified, and analyzed with the Lachat system at the end of the cruise.

## 3. Results

The cruise covered a wide range in surface water conditions (Table 1). Variations in sea surface temperatures (SST) measured during the cruise ( $9\text{--}18^\circ\text{C}$ , Fig. 1a) were



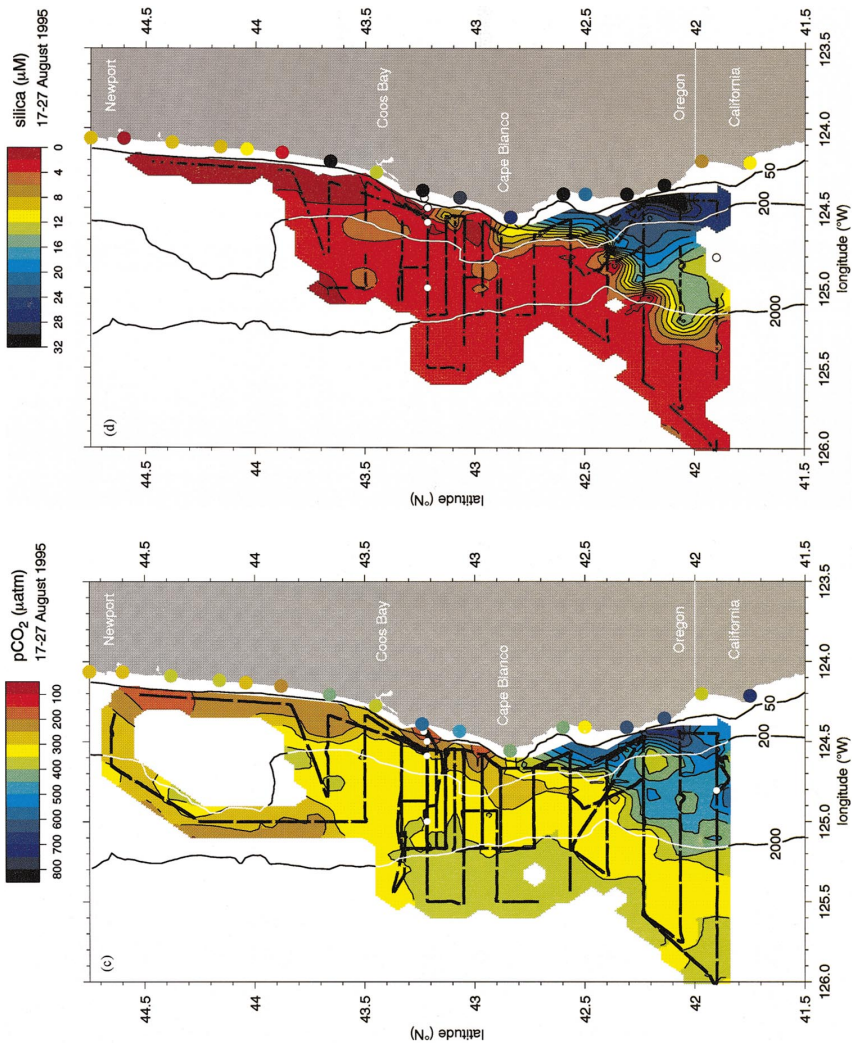


Fig. 1. Colored contours of surface (a) temperature, (b) salinity, (c)  $pCO_2$  at SST, and (d) silicate concentrations measured during August 17–27, 1995 cruise. Colored circles along coastline show surf-zone data on same color scale for samples collected August 25 and 26, 1995 (Appendix A). The surf-zone data were not used in contouring. White circles along 41.9° and 43.2°N indicate location of vertical profiles discussed in text. Isobaths in meters.

determined mainly by variations in the proportion of recently upwelled water. SSTs below  $\sim 15^{\circ}\text{C}$  over the shelf indicate that coastal upwelling was active throughout the cruise area. This is consistent with wind patterns measured on the coast at Newport ( $44.6^{\circ}\text{N}$ ) and Cape Arago ( $43.3^{\circ}\text{N}$ ); equatorward winds averaged 5 m/s at both locations between August 17–27, 1995 (Barth et al., 2000). A week of poleward winds preceded the cruise, the fourth of similar downwelling intervals since the spring transition in early May. Surface currents measured by ADCP (Fig. 2a) and surface dynamic heights calculated from the SeaSoar CTD data (Barth et al., 2000) indicate that a southward-flowing jet following the  $15^{\circ}\text{C}$  surface isotherm separated warm offshore water from cold inshore water. The jet accelerates from about 50 cm/s at a distance of 30 km west of Cape Blanco to 100 cm/s 100 km offshore of the Oregon-California border (Fig. 2a). A broader region of low SSTs indicates particularly strong upwelling south of Cape Blanco. Barth et al. (2000) attribute this intensification to conservation of potential vorticity as the current flows around the cape (Arthur, 1965). The wide range in salinity measured on board ship (31.0 to 33.8, Fig. 1b) is the combined result of dilution by run-off from the north and upwelling of saltier water towards the coast (Huyer, 1983). Large deviations in salinity of water in the northwest corner of the cruise area from a broadly linear temperature-salinity relation for most surface waters reflect the direct influence of the Columbia River (Figs. 1b and 3a). Comparison of salinity profiles collected offshore at  $43.2^{\circ}\text{N}$  and  $41.9^{\circ}\text{N}$  indicates that upwelling affected the structure of the water column south of Cape Blanco to a depth of 100–150 m at a distance of 45 km from the coast (Fig. 4).

Surface water  $\text{PCO}_2$  measured during the cruise ranged from 150–700  $\mu\text{atm}$  (Fig. 1c). Over the range of conditions encountered during the cruise,  $\text{PCO}_2$  is determined mostly by the concentration of carbon dioxide ( $\text{TCO}_2$ ) in surface water. Other factors, in decreasing order of importance, are temperature, alkalinity, and salinity (Takahashi et al., 1980). In warm surface waters offshore of the jet, surface  $\text{PCO}_2$  levels converge to equilibrium with the atmosphere (Figs. 1c and 3b). Inshore of the jet, surface water  $\text{PCO}_2$  levels were generally undersaturated relative to the atmosphere (360  $\mu\text{atm}$ ) north of Cape Blanco, and supersaturated to the south. Variations in surface water  $\text{PCO}_2$  were accompanied by changes in nutrient concentrations across all ship tracks. In an area south of Cape Blanco were  $\text{PCO}_2$  levels were particularly high, P, Si, and  $\text{NO}_3$  concentrations in surface waters reached levels of 1.8, 33, and 23  $\mu\text{mol/kg}$ , respectively (Figs. 1d and 3c–e). Comparable P and Si concentration were measured at 80 m depth at the offshore profile south of Cape Blanco (Fig. 3c, d). Within a band of surface water with  $\text{PCO}_2$  levels down to 150  $\mu\text{atm}$  north of Cape Blanco, P, Si, and  $\text{NO}_3$  concentrations were reduced to levels below their detection limits of 0.1, 0.2, and 0.1  $\mu\text{mol/kg}$ , respectively. In the case of P and Si, these concentrations are lower than in warm surface waters offshore (Fig. 3c, d).

At the low end of its dynamic range,  $\text{PCO}_2$  provides more information than nutrients because of the reference provided by gas exchange equilibrium with the atmosphere. Under typical oceanic conditions, the time scale for equilibration of a 75-m-thick surface mixed layer with the atmosphere is about one year for  $\text{CO}_2$ , ten times slower than for  $\text{O}_2$  (Broecker and Peng, 1982). Surface mixed layers in upwelling systems are often only 10 m deep. Since both input of  $\text{CO}_2$ -enriched water from below



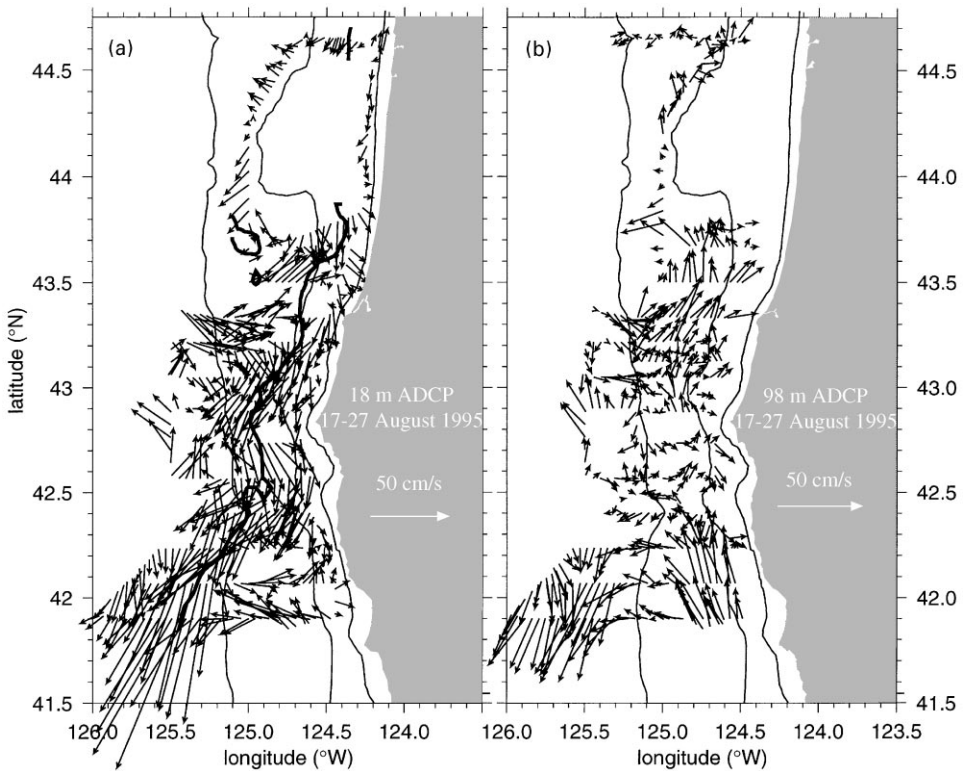
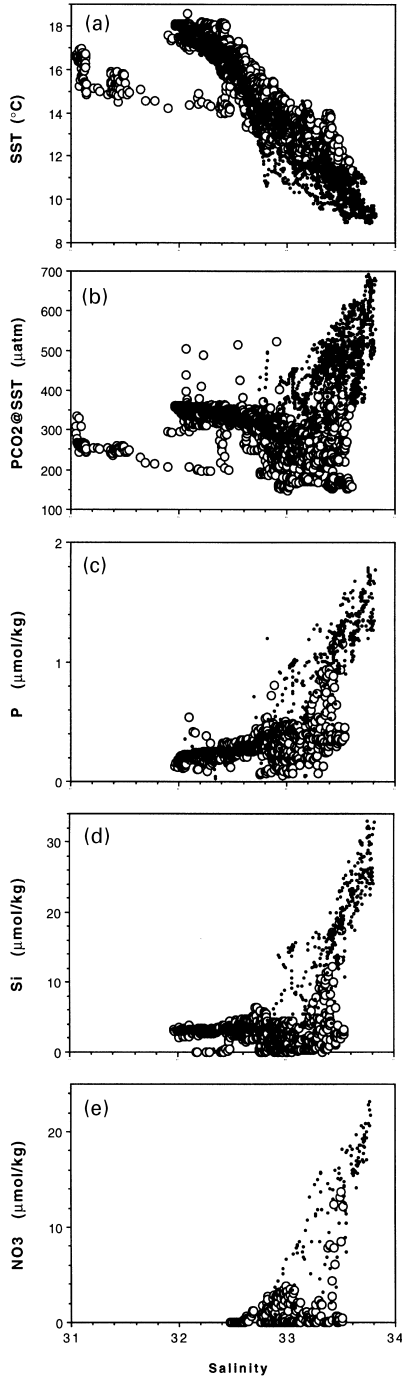


Fig. 2. Vector plots of ADCP data collected throughout the cruise at (a) 18 m and (b) 100 m depth. Thin lines show 50, 200, and 2000 m isobaths. Thick line in (a) shows location of upwelling front as indicated by 15°C surface isotherm.

and warming of this thin layer would tend to increase  $\text{PCO}_2$ , the extremely low levels observed over the continental shelf north of Cape Blanco are an unambiguous indication of  $\text{CO}_2$  drawdown by phytoplankton (Fig. 1c). Drawdown is also indicated by  $\text{PCO}_2$  levels and nutrient concentrations in surface waters north of Cape Blanco that are much lower than in surface waters south of Cape Blanco at equal salinity (Fig. 3b–d). The sharp contrast in surface  $\text{PCO}_2$  levels north and south of Cape Blanco within the 200 m isobath indicates a different biological response to upwelling in the two regions (Fig. 1c).

The range of tracer concentration measured in surf-zone samples collected August 25 and 26 is similar to that measured on board ship (Table 1). The composition of nearshore surface water sampled from the ship during the second half of the cruise (August 21–27) within a distance of 10–40 km from the coast is compared to surf-zone properties in Fig. 5. North of Cape Blanco,  $\text{PCO}_2$ , P and Si levels in the surf-zone were considerably higher than in shelf waters analyzed on board ship (Fig. 5d–f). Surf-zone and shelf water at the same latitude were similar in composition south of Cape Blanco. North–south gradients in surf-zone  $\text{PCO}_2$ , Si and P are consistent with



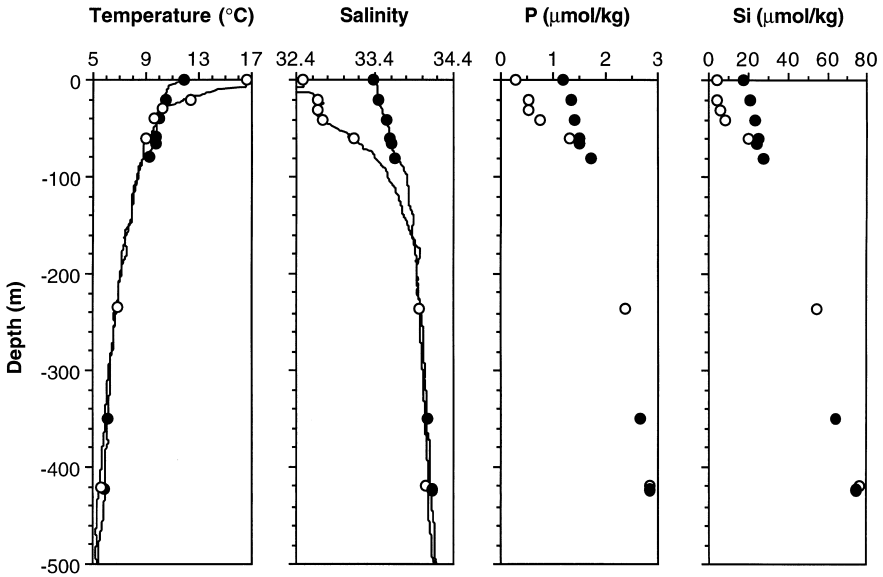


Fig. 4. Comparison of water column profiles at two offshore stations (Appendix B) 46 km from the coast at 41.9°N (filled circles) and 43.2°N (open circles). CTD data at the two stations indicated by solid lines.

Table 1  
Comparison of range in surface water properties

	Ship	Surf-zone
SST (°C)	9.0–18.2	10.7–16.0
Salinity	31.0–33.8	31.7–33.8
PCO <sub>2</sub> @SST (µatm)	150–690	250–640
P (µmol/kg)	< 0.1–1.8	0.3–2.0
Si (µmol/kg)	< 1–33	1.1–42
TCO <sub>2</sub> (µmol/kg)	1890–2160	1980–2120
Alkalinity (µeq/kg)	2240–2260	n.d. <sup>a</sup>

<sup>a</sup> n.d.-not determined.

the southward increase in upwelling intensity indicated by shipboard SST. Both the shipboard and the surf-zone data indicate particularly strong upwelling at ~ 42.2°N (Fig. 5d–f). The region of elevated P and Si concentrations in the surf-zone extended about 100 km further north (~ 43.3°N) than in the nearshore waters sampled by ship.

←  
Fig. 3. (a) Temperature, (b) PCO<sub>2</sub>@SST, (c) phosphate, (d) silicate and (e) nitrate as a function of salinity measured underway. Samples north and south of Cape Blanco (42.8°N) are shown by large open circles and filled small circles, respectively. The data include ~ 8000 individual measurements of PCO<sub>2</sub>, 1700 measurements of P and Si, and 400 of NO<sub>3</sub>.

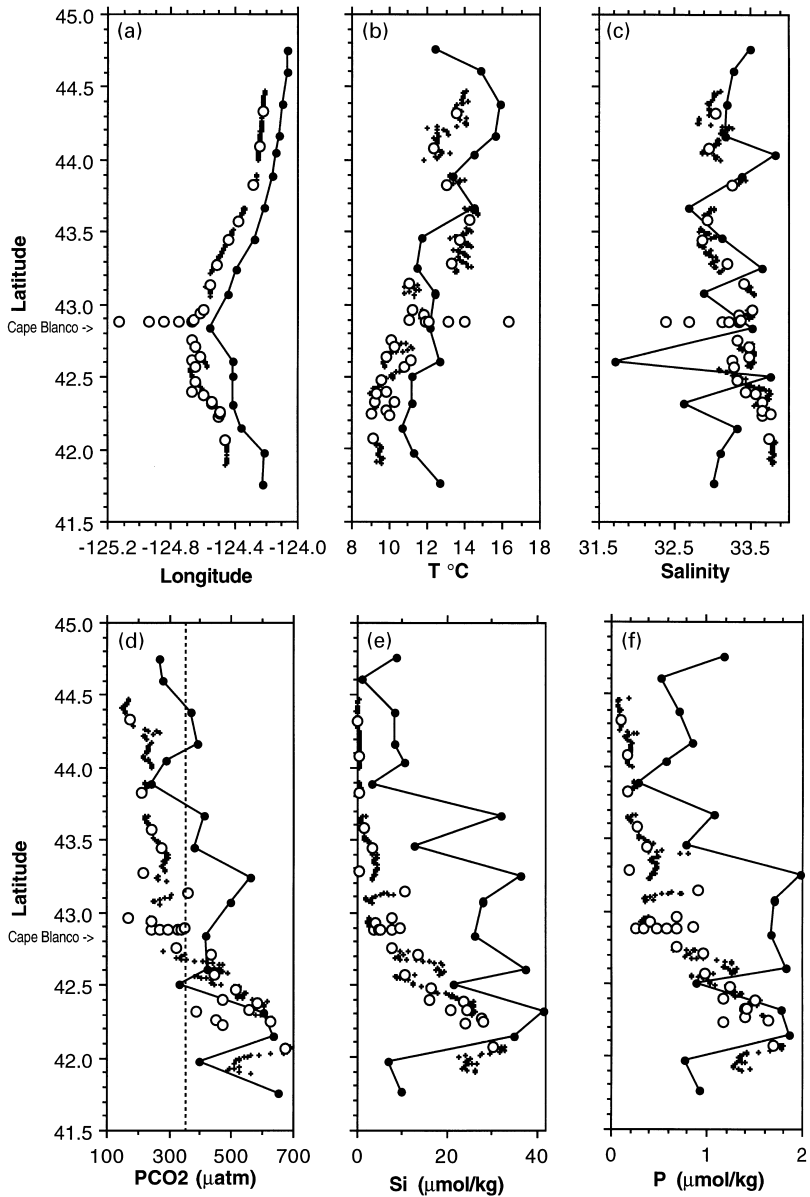


Fig. 5. Comparison of shipboard nearshore transect (small crosses) and beach transect (filled circles) for (a) position, (b) T, (c) S, (d)  $\text{PCO}_2@SST$ , (e) Si, and (f) P. Open circles indicate samples with additional carbonate system data (Appendix, Table A3).

This is because the coastal upwelling front was close to coast north of Cape Banco; the ship encountered freshly upwelled water only south of Cape Blanco where the front separated from the shelf, allowing the freshly upwelled water to extend farther

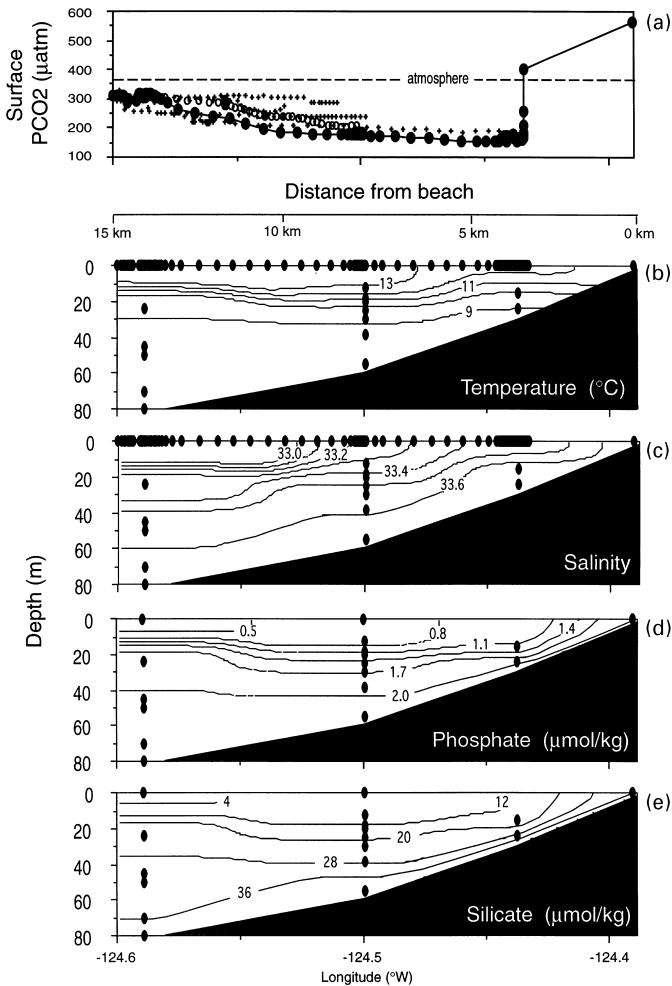


Fig. 6. Cross-shelf section from the surfzone to 15 km offshore at 43.2°N (Table 3): (a) Surface PCO<sub>2</sub> at in situ T, (b) T section, (c) S section, (d) P section, (e) Si section. Sample locations indicated by filled circles. The vertical profiles and surface PCO<sub>2</sub> data indicated by solid circles were all collected on August 18 and 19, 1995, with the exception of the surf-zone sample collected on August 25. Small crosses show additional surface PCO<sub>2</sub> data collected on August 18, 24 and 27 within 10 km north and south of the profiles. Open circles show PCO<sub>2</sub> data collected in the same region on August 26, one day after the surf-zone sample was collected.

seaward. Salinity and temperature are more ambiguous indicators of upwelling. There is no systematic pattern in surf-zone salinity, most likely because the effect of variations in local run-off dominates; dilution with less than 10% of fresh water could explain the variations in salinity (Fig. 5c). Although surf-zone water temperatures were generally higher than offshore, the north–south temperature gradient was more consistent with the other upwelling indicators than salinity. The trend of southward

decrease in surf-zone temperature from  $\sim 16$  to  $11^\circ\text{C}$  roughly parallels an alongshore decrease in SST from  $14$  to  $9^\circ\text{C}$  measured on board ship (Fig. 5b).

In order to establish the nearshore distribution of upwelling source waters, chemical parameters were measured in samples collected by Niskin bottle casts across the shelf on August 18 and 19 at  $43.22^\circ\text{N}$  latitude (Appendix, Table A2). These profiles, supplemented with a surf-zone sample collected at  $43.24^\circ\text{N}$  on August 25, were used to draw contours of temperature, salinity, P, and Si for the inner 15 km of the shelf (Fig. 6).  $\text{PCO}_2$  measured at the time the profiles were collected shows that surface waters over the shelf were highly undersaturated relative to the atmosphere, with a few exceptions near shore (Fig. 6a). Surface concentration of nutrients are poorly constrained along this particular transect because the towed pumping device was not deployed between casts. But surface P and Si concentrations measured on the same day between  $124.5$  and  $125.6^\circ\text{W}$  and within a distance of 10 km from the transect of profiles were very low:  $0.2 \pm 0.03$  and  $0.4 \pm 0.2 \mu\text{mol/kg}$ , respectively ( $n = 15$ ).  $\text{PCO}_2$  data collected before and after the casts including August 26, the day before the surf-zone sample was collected, show persistent undersaturation relative to the atmosphere over the shelf (Fig. 6a). Additional surf-zone samples collected at the same latitude contained 1.9 and  $2.0 \mu\text{mol/kg}$  P and 31 and  $33 \mu\text{mol/kg}$  Si on August 23 and September 15, respectively (R. Takesue and A. van Geen, in preparation). These observations, combined with a small number of shipboard determinations showing elevated  $\text{PCO}_2$  on August 19 at a distance of 3 km from the coast, suggest that the sharp front separating supersaturated water extending from the surf-zone and undersaturated surface water over the shelf is a fairly persistent feature. The salinity and nutrient content of surf-zone water was similar to that of near-bottom water at a depth of 60–70 m, 15 km from the coast, as well as water from  $\sim 100$  m depth at a distance of 45 km from the coast (Figs. 4 and 6).

$\text{TCO}_2$  and alkalinity were measured for a set of discrete surface samples collected on board ship and in the surf-zone (Appendix, Tables A1, A3). The shipboard surface samples were collected mostly nearshore over a wide range in conditions (Fig. 5a). Carbonate parameters also were measured for Niskin bottle samples from three vertical profiles (Appendix, Table A2) two at  $43.2^\circ\text{N}$  (3.6 and 8.2 km from the coast) and one at  $41.9^\circ\text{N}$  (45 km). The profile data show a linear relation between  $\text{TCO}_2$  and P (Fig. 7a) that is consistent with the relation between these parameters for surface samples collected from the ship in supersaturated and undersaturated waters. This suggests that the composition of coastal diatoms in this area is not very different from the world average. In contrast to surface waters collected on board ship, the carbon and P content of about half the surf-zone samples deviates from the linear relation defined by the offshore samples (Fig. 7a).

## 4. Discussion

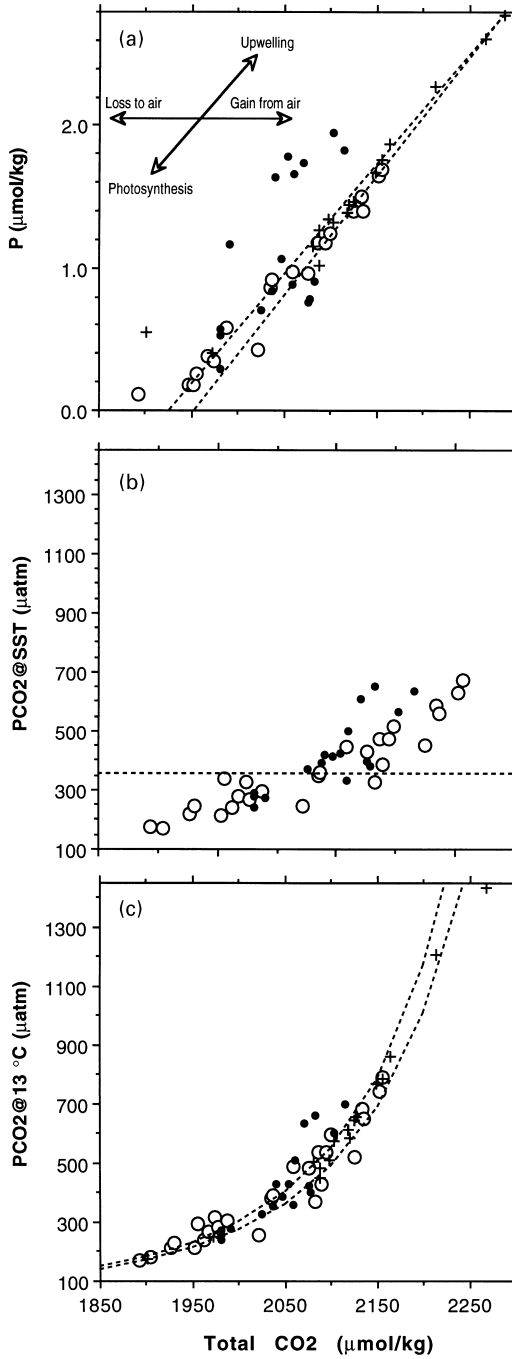
### 4.1. Carbon and nutrients

$\text{PCO}_2$  is a property of seawater determined by circulation and biology.  $\text{PCO}_2$  is also particularly amenable to continuous shipboard analysis. No reagents are needed,

and a gas cylinder contains enough standard gas for months of operation. For these reasons, and because of the importance of the carbon cycle for climate, factors controlling surface  $\text{PCO}_2$  in the open ocean have been studied for several decades (Greenberg et al., 1932; Buch et al., 1932; Broecker and Takahashi, 1966; Takahashi et al., 1993). There have been fewer systematic studies of  $\text{PCO}_2$  in nearshore waters despite the importance of continental shelf processes of the carbon cycle, however. Our data from the Cape Blanco area show that  $\text{PCO}_2$  is a particularly sensitive and convenient tracer of coastal upwelling. The downside of  $\text{PCO}_2$ , i.e. sensitivity to  $\text{TCO}_2$ , T, alkalinity, and S over the range of surface conditions encountered during the cruise, is shown graphically in Fig. 8. Although variations in  $\text{TCO}_2$  clearly account for most of the variations in surface  $\text{PCO}_2$  measured during the cruise, the combined effect of T and S over conditions encountered during the cruise can vary  $\text{PCO}_2$  by an amount equivalent to 1/4 of the dynamic range of  $540 \mu\text{atm}$ . Underway T and S measurements generally do not pose a problem; this is not the case for alkalinity, which must be measured on discrete samples in the laboratory. The range in surface alkalinities encountered during the cruise can vary  $\text{PCO}_2$  by an amount equivalent to 6% of the dynamic range (Fig. 8).

Since  $\text{PCO}_2$  depends on several factors other than  $\text{TCO}_2$ , some scatter is expected in a plot of  $\text{PCO}_2@SST$  vs.  $\text{TCO}_2$  for samples collected on board shipboard and in the surf-zone (Fig. 7b). The scatter is considerably reduced when  $\text{PCO}_2$  values at SST are converted to  $\text{PCO}_2$  at a constant temperature of  $13^\circ\text{C}$  to remove the effect of differences in temperature (Fig. 7c). Alkalinity and nutrients concentrations are not required to apply the empirical relation between  $\text{PCO}_2$  and T used in these calculations (Takahashi et al., 1993). The exponential increase in  $\text{PCO}_2$  as a function of  $\text{TCO}_2$ , intrinsic to the nature of carbonic acid dissociations in seawater, explains why  $\text{PCO}_2$  is such a sensitive indicator of upwelling.  $\text{PCO}_2$  at  $13^\circ\text{C}$  calculated for all subsurface samples follows the sample exponential relation to  $\text{TCO}_2$  (Fig. 7c). The remaining scatter in the  $\text{TCO}_2$ - $\text{PCO}_2@13^\circ\text{C}$  plot cannot be attributed solely to alkalinity differences among samples since the maximum possible effect over the range of surface  $\text{TCO}_2$  concentrations is on the order of  $\pm 16 \mu\text{atm}$  (Fig. 8). Given the spatial variability of chemical properties in nearshore waters, this scatter is most likely due to a mismatch in composition between discrete samples taken from the ship's seawater supply and the equilibrator  $\text{PCO}_2$  measurement.

$\text{NO}_3$  concentrations as high as  $25 \mu\text{mol/kg}$  were measured in surface waters during the cruise (Fig. 3c).  $\text{NO}_3$  uptake by phytoplankton in the bloom area north of Cape Blanco therefore could have raised the alkalinity of surface water by as much as  $25 \mu\text{eq/kg}$ . A useful conservative property for determining mixing relationships between different water masses is therefore "potential alkalinity" ( $\text{NO}_3$  + alkalinity, Brewer and Goldman, 1976). It is equivalent to the alkalinity reached by a sample after all  $\text{NO}_3$  has been removed. The relation between potential alkalinity and  $\text{TCO}_2$  is shown for all surface and profile samples in Fig. 9a. For samples collected when the underway  $\text{NO}_3$  system was not operating, potential alkalinity was calculated by estimating  $\text{NO}_3$  from the near-linear relation to P concentrations. The data indicate that a linear relation between  $\text{TCO}_2$  and potential alkalinity at depth can be largely explained by conservative mixing of two end-members (Fig. 9a). Nearshore surface





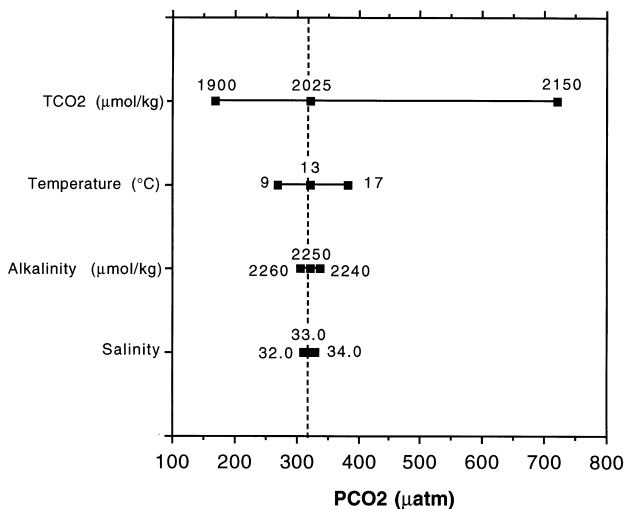


Fig. 8. Sensitivity of PCO<sub>2</sub> to changes in TCO<sub>2</sub>, T, alkalinity, and S over the range of conditions encountered during the cruise (Table 1).

waters in the bloom area deviate from this relation because their potential alkalinity is essentially constant ( $2250 \pm 20 \mu\text{eq/kg}$ , Fig. 9a). This indicates that the phytoplankton bloom north of Cape Blanco contains few calcite-secreting organisms such as foraminifera or coccoliths. Although samples were not preserved during the cruise for plankton identification, the chemical data are consistent with other studies indicating that nearshore blooms in coastal waters of the California Current are dominated by large diatoms (Chavez et al., 1991; Hood et al., 1991). Potential alkalinity provides, therefore, a measure of the initial TCO<sub>2</sub> concentration in upwelled water. Based on this reasoning, it appears that up to 200  $\mu\text{mol/kg}$  TCO<sub>2</sub> was removed by phytoplankton in the area of most intense drawdown (Fig. 9a).

Two offshore surface samples that have a low salinity due to an addition of Columbia River water extend the linear relation between potential alkalinity and TCO<sub>2</sub> defined by subsurface samples (Fig. 9a). A plot of potential alkalinity as a function of salinity for both surface and deep samples helps to explain this relation (Fig. 9b). The data show that most of the variations in potential alkalinity in the region can be explained by dilution of saline and alkaline deep waters with fresh

Fig. 7. Property plots (a) P, (b) PCO<sub>2</sub>@SST, (c) PCO<sub>2</sub>@13°C as a function of TCO<sub>2</sub>. Surface samples collected on board ship indicated by open circles; surf-zone samples by closed circles. Crosses show data for profiles samples with carbonate data. Two dashed lines in (a) originate at deepest profile sample with C/P slopes of 120 and 130, respectively. Dashed line in (b) shows atmospheric PCO<sub>2</sub> measured during the cruise. Two dashed lines in (c) show PCO<sub>2</sub>@13°C calculated from TCO<sub>2</sub> and alkalinities of 2240 and 2260  $\mu\text{eq/kg}$ , respectively.

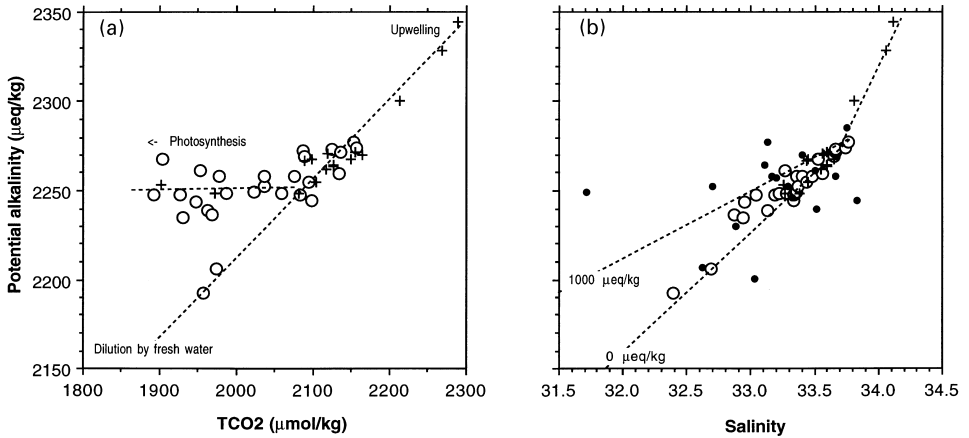


Fig. 9. Potential alkalinity as function of (a)  $\text{TCO}_2$  and (b) salinity. Open circles indicate surface samples collected on board ship, crosses indicate profile samples, filled circles indicate surf-zone samples. Dashed lines in (b) labelled “1000  $\mu\text{eq/kg}$ ” and “0  $\mu\text{eq/kg}$ ” indicate dilution trends with freshwater at these alkalinities.

water. The scatter in the data is encompassed by a fresh water end-member ranging between 0  $\mu\text{eq/kg}$  (i.e. precipitation) and 1000  $\mu\text{eq/kg}$ , which is comparable to Columbia River water alkalinity of about 1200  $\mu\text{eq/kg}$  (Berner and Berner, 1987). The two corresponding dilution lines in Fig. 9b originate at the most saline and alkaline sample collected on board ship. This analysis suggests that the detailed mixing and biological history of a parcel of upwelled water could be reconstructed by using potential alkalinity–salinity and potential alkalinity– $\text{TCO}_2$  relations. Comparison of the highest potential alkalinities measured in surface waters (2270–2280  $\mu\text{eq/kg}$ ) suggests a maximum depth of origin of 100–150 m relative to the offshore profile south of Cape Blanco, 45 km from the coast.

The surf-zone samples exhibit considerably more scatter in the relation between potential alkalinity and salinity (Fig. 9b). Considering the reproducibility of our alkalinity measurements discussed earlier, the scatter is unlikely to be analytical. The scatter however could be an artifact produced by precipitation/dissolution reactions involving particles that were trapped in the surf-zone sample bottles. In contrast, deviations of the  $\text{TCO}_2$  and P content of surf-zone water from the systematic relation seen for offshore surface water are probably a real feature (Fig. 7a). There is a considerable  $\text{TCO}_2$  deficit for the 7 samples containing the highest contributions of freshly upwelled water ( $P > 1.2 \mu\text{mol/kg}$ , Fig. 7a). A simple calculation shows this could be due to enhanced gas exchange in the surf-zone. The net flux of  $\text{CO}_2$  between seawater and air can be estimated by the relation:  $F(\text{sw-a}) = E(\text{PCO}_{2,\text{sw}} - \text{PCO}_{2,\text{a}})$ , where  $E$  is the gas transfer coefficient. The dependence of gas transfer on wind speed can be approximated on the basis of  $^{14}\text{C}$  distribution in air and ocean water (Broecker et al., 1986; Tans et al., 1990) by  $E(\text{mol CO}_2 \text{ m}^{-2} \text{ yr}^{-1}) = 0.016. [W (\text{m s}^{-1}) - 3]$  for  $W > 3 \text{ m s}^{-1}$ . Breaking

waves are likely to enhance gas exchange in the surf-zone. If this enhancement is assumed to be comparable to wave conditions in the open ocean under 40 knots of wind ( $20 \text{ m s}^{-1}$ ), the flux of  $\text{CO}_2$  into the atmosphere corresponding to a  $300 \mu\text{atm}$  supersaturation (Fig. 7b) is  $86 \text{ mol CO}_2 \text{ m}^{-2} \text{ yr}^{-1}$ . At this rate, the loss of  $\sim 50\text{--}100 \mu\text{mol/kg TCO}_2$  from the surf-zone suggested by anomalies relative to P (Fig. 7a) could be achieved in 5–10 h, assuming a 1 m mixed layer of surf-zone water. Degassing of initially supersaturated surf-zone samples could therefore explain the deviations from the  $\text{TCO}_2\text{--P}$  relation in Fig. 7a.

#### 4.2. Surface circulation and the biological response to upwelling

Two high-resolution transects at  $42^\circ$  and  $43^\circ\text{N}$  characteristic of contrasting conditions north and south of Cape Blanco were selected for closer comparison with the ADCP data (Fig. 10). Surface temperature and salinity gradients across the jet are comparable in both transects (Fig. 10b and c). Most of the water advected southward by the jet is nutrient-depleted and slightly undersaturated with respect to atmospheric  $\text{PCO}_2$  (Fig. 10d–f). At both  $42^\circ$  and  $43^\circ\text{N}$ , the inshore margin of the jet is marked by an increase in surface  $\text{PCO}_2$  and local nutrient maxima. The coastal jet therefore forms a boundary between upwelled water inshore and oceanic water offshore. This is consistent with observations from previous experiments (Huyer et al., 1991; Chavez et al., 1991) that waters advected by the coastal jet are fresher and lower in nutrients than water inshore of the local coastal upwelling front. Our data show that when the coastal jet separates from the shelf, upwelled water is allowed to extend across the shelf break (Fig. 1; Barth et al., 2000). The main chemical difference between the two transects is the strong bloom indicated by low  $\text{PCO}_2$  levels at  $43^\circ\text{N}$  located just offshore of the inshore margin of the coastal jet (Fig. 10d). There is a local maximum in surface temperature centered on the region of reduced surface  $\text{PCO}_2$  and nutrient concentrations (Fig. 10b). At  $42^\circ\text{N}$ , the relation between a local maximum in temperature and a local minimum in surface  $\text{PCO}_2$  at roughly the same longitude is even better defined ( $124.6^\circ\text{W}$ , Fig. 10b and d). Surface ADCP data indicate that the  $\text{PCO}_2$  minimum of the southern transect is probably an extension of the same bloom entrained with the cyclonic gyre on the inshore side of the coastal jet south of Cape Blanco (Fig. 2a, see also Barth et al., 2000). A northern source for the  $\text{PCO}_2$  minimum at the southern transect and an inshore reversal of flow (Fig. 10a) is consistent with the low salinity of this feature (Fig. 10c).

Data from a large number of cruises off the Oregon coast show that the phytoplankton bloom located over Heceta Bank, the shelf extension southwest of Newport (Fig. 1), is a recurrent feature (Small and Menzies, 1981; Landry et al., 1989). An 8-year composite of Coastal Zone Color Scanner data for August also shows an area of elevated pigment concentrations that extends over Heceta Bank and becomes much narrower further south (Thomas et al., 1994). As in the case of the filaments of elevated pigment concentrations that extend offshore further south in the California Current (Strub et al., 1991), the bloom over Heceta Bank appears to be linked to topography. The positive temperature anomalies associated with the phytoplankton bloom (Fig. 10) suggest that the development of a bloom requires some time after upwelled

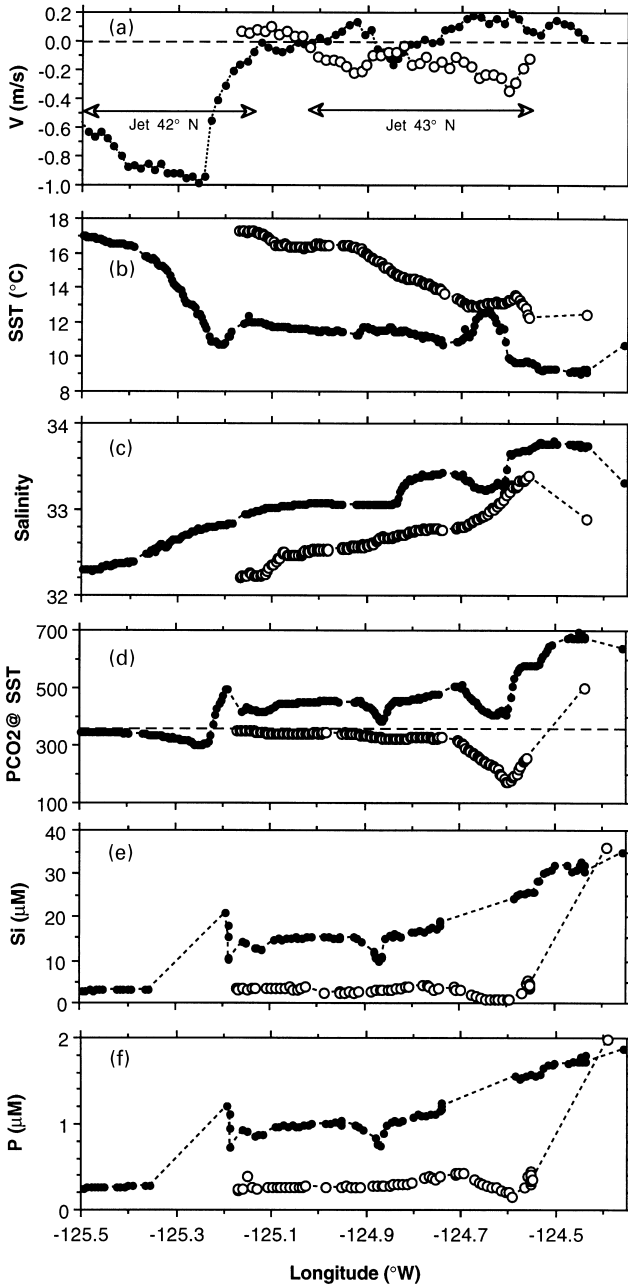


Fig. 10. Cross-shelf transects of surface (a) current velocity measured by ADCP (+ north), (b) T, (c) S, (d)  $\text{PCO}_2@SST$ , (e) Si, and (f) P at 42.0° (solid circles) and 43.0°N (open circles). Surfzone samples at both latitudes indicated by symbol furthest east. Dashed lines connect shipboard and surf-zone data sets across regions not reached by ship or, additionally for Si and P, regions where nutrient data were not collected.

water reaches the surface during which surface water will warm. Lagrangian studies of coastal upwelling plumes off Peru and California also have shown that there can be a considerable delay in response of coastal diatoms to upwelling (MacIsaac et al., 1985; Wilkerson and Dugdale, 1987). There is evidence of water retention within the bloom area north of Cape Blanco. A surface drifter tracked by satellite released inshore of the coastal jet at 43.5°N on August 19, 1995 remained in the same area for several weeks and ran ground just south of Cape Blanco on September 15, 1995 (Barth et al., 2000). The available data therefore suggest that a bloom may not have developed south of Cape Blanco because of more vigorous circulation in the area. The recent demonstration that low Fe levels can limit phytoplankton growth off California (Hutchins and Bruland, 1998) suggests that coastal topography may play an additional role in regulating phytoplankton growth through its effect on Fe input to nearshore waters (Landing and Bruland, 1987; Martin and Gordon, 1988).

#### 4.3. Circulation at depth and the origin of surf-zone water

T–S and Si–S relations for the three shelf profiles at 43.2°N, the offshore profile at this latitude, and three bottom-water samples collected in between (21, 27, and 33 km from the coast, Table 2) are compared in Fig. 11. The data show that the T–S relation of all bottom water samples is consistent within  $\pm 0.2^\circ\text{C}$  with the offshore profile up to a distance of 4 km from the coast (Fig. 11a). Not surprisingly, the temperature of the shallowest profile samples and surf-zone water was elevated relative to the T–S relation of offshore profile due to heat exchange across the sea surface (Fig. 11a). The Si–S relations of bottom water samples as well as surf-zone water inshore of the transect are also consistent with the offshore profile (Fig. 11b). This suggests a connection between the surf-zone and water masses over the shelf floor that is consistent with ADCP-derived onshore currents at depth over the shelf in most of the cruise area (Fig. 2b). Onshore advection at depth over the inner shelf during upwelling has recently been modeled (Allen et al., 1995) and observed with current moorings

Table 2  
Composition of bottom water advected across the shelf

Lat (°N)	Long (°W)	Distance from coast	Bottom depth	Sample depth	T	S	P	Si
43.240	124.390	0	0	0	11.47	33.658	1.99	36.4
43.232	124.437	4	30	24	8.76	33.661	2.04	29.9
43.217	124.499	8	60	55	8.11	33.793	2.28	43.6
43.217	124.599	15	82	80	7.98	33.799	2.23	43.7
43.233	124.666	21	155	140	7.65	33.902	2.29	49.6
43.216	124.751	27	315	295	6.97	34.001	2.41	54.2
43.217	124.835	33	345	325	6.27	34.012	2.53	62.3
43.217	124.999	46	xxx	420	5.93	34.120	2.78	74.9

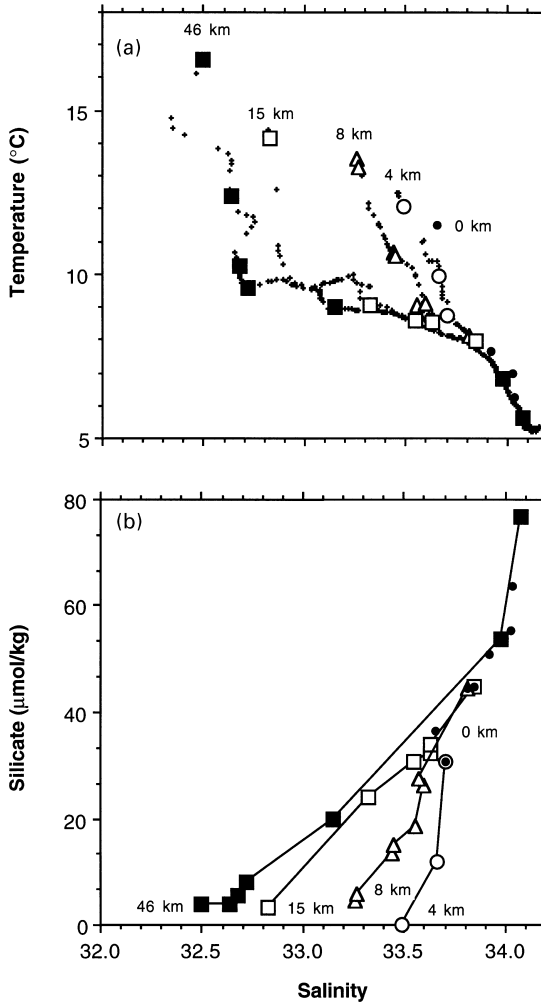


Fig. 11. (a) Temperature and (b) Si as a function of salinity for Rosette samples collected along 43.2°N (Table 3). CTD data indicated by individual crosses at 1-m-depth intervals. Superimposed as filled circles are all bottom water samples listed in Table A3.

deployed nearshore (Huyer, 1983; Lentz, 1994). Salinity, nutrients, and potential alkalinity indicate a depth of origin for surf-zone water of 100–150 m depth at a distance of 45 km from the coast. Samples collected in August 1996 at 43.2°N containing 2.6 and 60  $\mu\text{mol/kg}$  P and Si, respectively, suggest surf-zone water can originate from even greater depths (R. Takesue and A. van Geen, in prep.) These observations are consistent with surf-zone data from Pillar Point, California, indicating P and Si concentrations of up to 2.4 and 48  $\mu\text{mol/kg}$  during the upwelling season (van Geen and Husby, 1996). In this study, depths of origin of about 250 and 320 m

were calculated relative to profiles located further offshore (100 and 200 km, respectively).

The composition of surfzone water at 43.2°N is similar to that measured for an additional five surf-zone locations further south. This is particularly evident for P, which is the upwelling-tracer least affected by local processes (Fig. 4f). Si concentrations are also elevated in the same samples ( $\sim 30 \mu\text{mol/kg}$ ), although there is higher variability among stations that is probably due to local run-off. Salinity depressions at 42.3° and 42.6°N, for instance, could add  $\sim 3$  and  $8 \mu\text{mol/kg}$  Si, respectively, based on the typical composition of run-off in the area ( $\sim 150 \mu\text{mol/kg}$ ). The distribution of salinity at depth suggests that the composition of source waters over the shelf is probably fairly uniform. At all latitudes of the SeaSoar surveys between 43.34° and 41.90°N, salinity below 55 m depth at the most inshore points was between 33.69 and 33.89 (J. Barth and R.L. Smith, unpubl. data). Hermann et al. (1989) showed that, during a period of coastal upwelling, the nutrient content of bottom water was homogeneous over a distance of 100 km along the Washington coast. Strong alongshore currents and intense mixing in the bottom boundary layer (Lentz and Trowbridge, 1991) probably contribute to maintaining such a consistent composition of bottom water over large spatial scales. The apparent connection between the surf-zone and shelf bottom water may therefore explain why spatial and temporal changes in surf-zone composition at selected locations appear to be tied to large-scale wind patterns rather than to local effects (van Geen and Husby, 1996). The relation between surf-zone composition and wind forcing breaks down, however, at locations where diatom growth is particularly intense over the shelf (e.g. north of 43.3°N and south of 42.1°N, Figs. 1d and 5e, f) or in the surf-zone further north along the Oregon and Washington coast.

## 5. Conclusions

The complex features of nearshore circulation during coastal upwelling can be resolved by continuous shipboard analyses of  $\text{PCO}_2$  and nutrients. These tracers complement temperature and salinity because they document the biological response to coastal upwelling, or lack thereof.  $\text{PCO}_2$  undersaturation relative to the atmosphere is an unambiguous indication of primary production caused by a phytoplankton bloom. The high-precision determination of potential alkalinity as a conservative tracer of upwelling opens up the possibility of determining the absolute level of  $\text{TCO}_2$  drawdown in a bloom.

Physical parameters measured off the coast of Oregon in August 1995 during a period of equatorward wind forcing indicate that a coastal jet that marked the upwelling front left the continental shelf near Cape Blanco and became an oceanic jet (Barth et al., 2000). Our chemical data collected during the same cruise indicate that Cape Blanco also marks a boundary between two areas of contrasting biological response to upwelling. A large phytoplankton bloom was concentrated over Heceta Bank and inshore of the coastal jet north of Cape Blanco. There was little indication of biological activity south of Cape Blanco. The precise origin of this contrast remains an open question.

Comparison of the composition of surf-zone water collected along the cruise area with a set of vertical profiles suggests efficient exchange with a bottom boundary layer over the inner continental shelf. Intense mixing within the bottom boundary layer and exchange with the surf-zone may explain why the composition of surf-zone water appears to be determined by large-scale wind patterns rather than local processes.

## Acknowledgements

We thank the crew of RV *Wecoma* and Marine Technician Marc Willis for support throughout the cruise. Laura Verhegge and Theresa McEvoy from the Oregon Institute of Marine Biology (Charleston, OR) collected the surf-zone samples. A.vG and R.K.T. were supported in part by ONR, J.G. and T.T. by NSF, J.A.B. and R.L.S. and ship time by NSF grant OCE 93-14370. We thank Steve Pierce (OSU) for processing the ADCP data. Stefan Petranek was supported by an ONR high-school fellowship to help with cruise preparations at L-DEO.

## Appendix

Table A1  
Surf-zone data collected on August 25–26, 1998

Name	Lat (°N)	Long (°W)	T (°C)	S	P ( $\mu\text{mol/kg}$ )	Si	PCO <sub>2</sub> ( $\mu\text{atm}$ ) <sup>a</sup>	TCO <sub>2</sub> ( $\mu\text{mol/kg}$ ) <sup>a</sup>	Alkalinity ( $\mu\text{eq/kg}$ )
Otter Rock	44.750	124.063	12.45	33.500	1.16	8.7	271	1990	2249)2254
South Beach	44.600	124.065	14.85	33.287	0.53	1.1	282/278	1980	(2250)2247
Beachside	44.380	124.089	15.95	33.194	0.70	8.4	371	2025	(2252)2250
Washburne	44.160	124.117	15.65	33.169	0.84	8.1	399/390	2037	(2251)
Heceta Beach	44.040	124.132	14.50	33.829	0.57	10.5	292	1980	(2242)
Siltcoos	43.880	124.153	13.40	33.397	0.29	3.3	249/236	1980	(2270)
Zrolkovski	43.660	124.207	14.50	32.695	1.07	31.6	413	2046	(2242)
Horsefall	43.450	124.277	11.75	33.129	0.78	12.6	381	2078	(2272)
Seven Devils	43.240	124.390	11.47	33.658	1.95	35.6	562	2102	(2234)
Bandon	43.070	124.435	12.45	32.882	1.66	27.4	498	2061/2058	(2210)
Cape Blanco	42.840	124.558	12.20	33.519	1.63	25.5	416	2040	(2221)
Humbug	42.600	124.411	12.70	31.718	1.78	36.7	427/422	2054	(2228)
Nesika	42.500	124.411	11.20	33.755	0.88	21.0	338/324	2059	(2278)
Pistol River	42.310	124.411	11.25	32.624	1.74	40.8	607	2071	(2186)
Whaleshead	42.140	124.355	10.70	33.320	1.83	34.2	638/635	2116	(2224)
Wavecrest	41.970	124.204	11.30	33.109	0.76	6.8	395	2076	(2259)
Crescent city	41.750	124.214	12.70	33.026	0.91	9.8	652	2083	(2192)

<sup>a</sup>PCO<sub>2</sub> and TCO<sub>2</sub> values separated by “/” indicate replicate measurements on the same sample; alkalinity values in parentheses were calculated from PCO<sub>2</sub> measured in the field and TCO<sub>2</sub> measured in the laboratory.



Table A2  
Profile data

Depth (m)	Temperature (°C)	Salinity	P ( $\mu\text{mol/kg}$ )	S ( $\mu\text{mol/kg}$ )	TCO <sub>2</sub> ( $\mu\text{mol/kg}$ )	Alkalinity ( $\mu\text{eq/kg}$ )
43.232°N 124.437°W						
15	9.93	33.660	1.00	11.4	2088	2264
24	8.76	33.700	2.04	29.9		
43.217°N 124.499°W						
0	13.52	33.254	0.55	4.3	1902	2250
12	13.24	33.265	0.40	5.8	1972	2249
18	10.67	33.440	1.27	13.2	2088	2252
20	10.57	33.451	1.34	14.6	2098	2252
25	9.05	33.556	1.45	18.3	2199	2254
30	9.09	33.539	1.76	25.6	2155	2250
38	8.66	33.570	1.87	26.9	2163	2246
55	8.11	33.813	2.28	43.6	2214	2270
43.217°N 124.589°W						
0	14.13	32.824	0.39	3.0		
24	9.05	33.323	1.80	23.4		
45	8.58	33.549	1.97	30.2		
50	8.52	33.626	1.99	31.7		
70	8.54	33.630	2.02	33.1		
80	7.98	33.842	2.23	43.7		
43.217°N 124.999°W						
0	16.57	32.499	0.28	3.8		
20	12.39	32.640	0.51	3.9		
30	10.25	32.678	0.52	5.4		
40	9.59	32.718	0.72	7.7		
60	8.98	33.153	1.28	19.3		
235	6.82	33.974	2.32	52.6		
420	5.63	34.080	2.78	74.9		
41.902°N 124.805°W						
0	11.82	33.374	1.15	16.7	2081	2236
20	10.51	33.448	1.32	20.8	2104	2240
40	9.98	33.554	1.39	23.0	2118	2246
58	9.78	33.592	1.47	24.5	2127	2246
65	9.78	33.600	1.47	23.3	2126	2247/2245 <sup>a</sup>
80	9.23	33.650	1.67	27.2	2149	2247
350	6.16	34.064	2.61	62.9	2268	2293
423	5.93	34.120	2.78	73.3	2288	2306/2302 <sup>a</sup>

<sup>a</sup>Alkalinity values separated by “/” indicate replicate measurements on the same sample.

Table A3  
Discrete surface samples with carbonate data

Lat. (°N)	Long. (°W)	SST (°C)	Salinity	P ( $\mu\text{mol/kg}$ )	Si ( $\mu\text{mol/kg}$ )	PCO <sub>2</sub> @SST ( $\mu\text{atm}$ )	TCO <sub>2</sub> ( $\mu\text{mol/kg}$ )	Alkalinity ( $\mu\text{eq/kg}$ )
42.935	124.615	11.82	33.358	0.42	4.0	245	2022	2249
42.891	124.661	11.02	33.367	0.86	9.5	349	2036	2246
42.884	124.750	12.06	33.220	0.59	5.1	294	1987	2245
42.884	124.846	13.12	33.127	0.49	3.7	242	1962	2238
42.883	124.937	13.99	32.693	0.34	4.9	329	1974	2206
42.883	125.128	16.32	32.393	0.25	3.7	338	1956	2193
42.710	124.649	10.24	33.486	0.97	13.6	432	2076	2250
42.567	124.644	10.81	33.283	0.98	10.7	444	2058	2239
42.399	124.671	9.83	33.435	1.17	16.0	472	2094	2242
42.381	124.600	6.28	33.563	1.50	23.7	585	2134	2242
42.322	124.548	10.26	33.649	1.42	20.7	384	2090	2254
42.263	124.493	9.80	33.660	1.40	27.8	453	2125	2257
42.230	124.498	9.98	33.658	1.17	23.9	474	2086	2260
42.067	124.457	9.15	33.743	1.69	30.2	671	2156	2254
42.247	124.464	9.03	33.763	1.64	28.1	628	2153	2258
42.330	124.540	9.25	33.657	1.40	24.4	557	2136	2256/2254 <sup>a</sup>
42.473	124.647	9.60	33.332	1.24	16.4	517	2099	2231/2229 <sup>a</sup>
42.756	124.666	10.12	33.333	0.68	7.8	325	2082	2243/2240 <sup>a</sup>
42.885	124.668	11.91	33.351	0.68	7.8	268	1977	2254
42.967	124.598	11.21	33.526	0.68	7.8	170	1904	2263
43.135	124.552	11.03	33.406	0.92	10.7	359	2036	2250
43.277	124.513	13.28	33.192	0.20	0.4	218	1927	2248
43.443	124.441	13.71	32.871	0.38	3.4	278	1968	2236
43.576	124.376	14.30	32.937	0.28	1.4	244	1930	2235
43.831	124.282	13.02	33.262	0.18	0.3	211	1952	2262
44.085	124.245	12.37	32.954	0.18	0.4		1947	2244
44.331	124.224	13.60	33.037	0.11	0.1	176	1893	2248/2240 <sup>a</sup>

<sup>a</sup>Alkalinity values separated by “/” indicate replicate measurements on the same sample.

## References

- Allen, J.S., Newberger, P.A., Federiuk, J., 1995. Upwelling circulation on the Oregon continental shelf. Part I: Response to idealized wind forcing. *Journal of Physical Oceanography* 25, 1843–1866.
- Arthur, R.S., 1965. On the calculation of vertical motion in eastern boundary currents from determinations of horizontal motion. *Journal of Geophysical Research* 70, 2799–2803.
- Barber, R.T., Dugdale, R.C., MacIsaac, J.J., Smith, R.L., 1971. Variations in phytoplankton growth associated with the source and conditioning of upwelling water. *Investigation Pesquera* 35, 171–193.
- Barth, J.A., Pierce, S.D., Smith, R.L., 2000. A separating coastal upwelling jet at Cape Blanco, Oregon and its connection to the California Current System. *Deep-Sea Research II* 47, 783–810.
- Berner, E.K., Berner, R.A., 1987. *The Global Water Cycle, Geochemistry and Environment*. Prentice-Hall, Englewood Cliffs, NJ 397 pp.
- Brewer, P.G., Goldman, J.C., 1976. Alkalinity changes generated by phytoplankton growth. *Limnology and Oceanography* 21, 108–117.

- Broecker, W.S., Peng, T.H., 1982. Tracers in the Sea. Eldigio Press, Palisades, New York, 690 pp.
- Broecker, W.S., Takahashi, T., 1966. Calcium carbonate precipitation on the Bahama Banks. *Journal of Geophysical Research* 71, 1575–1602.
- Broecker, W.S., Ledwell, J.R., Takahashi, T., Weiss, R.F., Merlivat, L., Memery, L., Peng, T.H., Jahne, B., Munnich, K.O., 1986. Isotopic versus micrometeorological ocean CO<sub>2</sub> fluxes: a serious conflict. *Journal of Geophysical Research* 91, 10517–10527.
- Buch, K., Harvey, H.W., Wattenberg, H., Gripenberg, S., 1932. *Über das Kohlensäuresystem im Meerwasser*. Conseil Permanent International pour l'Exploration de la Mer, Rapports et Proces-Verbaux 79, 70 pp.
- Chavez, F., Barber, R.T., Kosro, P.M., Huyer, A., Ramp, S.R., Stanton, T.P., Rojas de Mendiola, B., 1991. Horizontal transport and the distribution of nutrients in the coastal transition zone off northern California: effects on primary production, phytoplankton biomass, and species composition. *Journal of Geophysical Research* 96, 14833–14848.
- Chelton, D.B., Bernal, P.A., McGowan, J.A., 1982. Large-scale interannual physical and biological interactions in the California Current. *Journal of Marine Research* 40, 1095–1125.
- Chipman, D.W., Marra, J., Takahashi, T., 1993. Primary production at 47°N and 20°W in the North Atlantic Ocean: a comparison between the <sup>14</sup>C incubation method and the mixed layer carbon budget. *Deep-Sea Research II* 40, 151–169.
- Greenberg, D.M., Moberg, E.G., Allen, E.g., 1932. Determination of carbon dioxide and titratable base in sea water. *Industrial and Engineering Chemistry, Analytical Edition* 4, 309–313.
- Hermann, A.J., Hickey, B.M., Landry, M.R., Winter, D.F., 1989. Coastal upwelling dynamics. In: Landry, M.R., Hickey, B.M. (Eds.), *Coastal Oceanography of Washington and Oregon*. Elsevier, Amsterdam.
- Hood, R.R., Abbott, M.R., Huyer, A., 1991. Phytoplankton and photosynthetic light response in the coastal transition zone off northern California in June 1987. *Journal of Geophysical Research* 96, 14769–14780.
- Hutchins, D.A., Bruland, K.W., 1998. Iron-limited diatom growth and Si: N uptake ratios in a coastal upwelling regime. *Nature* 393, 561–564.
- Huyer, A., 1983. Coastal upwelling in the California Current system. *Progress in Oceanography* 12, 259–284.
- Huyer, A., Kosro, P.M., Fleishbein, J., Ramp, S.R., Stanton, T., Washburn, L., Chavez, F.P., Cowles, T.J., Pierce, S.D., Smith, R.L., 1991. Currents and water masses of the coastal transition zone off northern California, June to August 1988. *Journal of Geophysical Research* 96, 14809–14831.
- Johnson, K.S., Petty, R.L., 1983. Determination of nitrate and nitrite in seawater by flow-injection analysis. *Limnology and Oceanography* 28, 1260–1266.
- Kosro, P., Huyer, A., Ramp, S.R., Smith, R.L., Chavez, F.P., Cowles, T.J., Abbott, M.R., Strub, P.T., Barber, R.T., Jessen, P., Small, L.F., 1991. The structure of the transition zone between coastal waters and the open ocean off northern California, winter and spring 1987. *Journal of Geophysical Research* 96, 14707–14732.
- Landing, W.M., Bruland, K.W., 1987. The contrasting bio-geochemistry of iron and manganese in the Pacific Ocean. *Geochimica et Cosmochimica Acta* 51, 29–43.
- Landry, M.R., Postel, J.R., Peterson, W.K., Newman, J., 1989. Broad-scale distribution of hydrographic variables on the Washington/Oregon shelf. In: Landry, M.R., Hickey, B.M. (Eds.), *Coastal Oceanography of Washington and Oregon*. Elsevier, Amsterdam.
- Lentz, S.J., 1994. Current dynamics over the northern California inner shelf. *Journal of Physical Oceanography* 24, 2461–2478.
- Lentz, S.J., Trowbridge, J.H., 1991. The bottom-boundary layer over the northern California shelf. *Journal of Physical Oceanography* 21, 1186–1201.
- MacIsaac, J.J., Dugdale, R.C., Barber, R.T., Blasco, D., Packard, T.T., 1985. Primary production cycle in an upwelling center. *Deep-Sea Research* 32, 503–529.
- Martin, J.H., Gordon, R.M., 1988. Northeast Pacific iron distribution in relation to phytoplankton productivity. *Deep-Sea Research* 35, 177–196.
- Peng, T.H., Takahashi, T., Broecker, W.S., Olafsson, J., 1987. Seasonal variability of carbon dioxide, nutrients, and oxygen in the northern North Atlantic: surface water: observations and a model. *Tellus* 39B, 439–458.

- Small, L.F., Menzies, D.W., 1981. Patterns of primary productivity and biomass in a coastal upwelling region. *Deep-Sea Research* 28A, 123–149.
- Strub, P.T., Kosro, P.M., Huyer, A., CTZ Collaborators, 1991. The nature of cold filaments in the California Current system. *Journal of Geophysical Research* 96, 14743–14768.
- Sverdrup, H.U., Allen, W.E., 1939. Distribution of diatoms in relation to the character of water masses and currents off southern California in 1938. *Journal of Marine Research* 2, 131–144.
- Sverdrup, H.U., Johnson, M.W., Fleming, R.H., 1942. *The Oceans: Their Physics, Chemistry, and General Biology*. Prentice-Hall, Englewood Cliffs, NJ, 1087 pp.
- Takahashi, T., Broecker, W.S., Werner, S.R., Bainbridge, A.E., 1980. Carbonate chemistry of surface waters of the world oceans. In: Goldberg, E.D., Horibe, Y., Saruhashi, K. (Eds.), *Isotope Marine Chemistry*. Uchidarokaku-ho Publications, Tokyo.
- Takahashi, T., Goddard, J., Chipman, D.W., Sutherland, S.C., Mathieu, G., 1991. Assessment of carbon dioxide sink/source in the North Pacific Ocean: seasonal and geographic variability, 1984–1989. Final Technical Report for Cont. 19X-SC428C, Department of Energy, Lamont-Doherty Geological Observatory, Palisades, New York, 157 pp.
- Takahashi, T., Olafsson, J., Goddard, J.G., Chipman, D.W., Sutherland, S.C., 1993. Seasonal variation of CO<sub>2</sub> and nutrients in the high-latitude surface oceans: a comparative study. *Global Biogeochemical Cycles* 7, 843–878.
- Tans, P.P., Fung, I.Y., Takahashi, T., 1990. Observational constraints on the global atmospheric CO<sub>2</sub> budget. *Science* 247, 1431–1438.
- Thomas, A.C., Huang, F., Strub, P.T., James, C., 1994. A comparison of the seasonal and interannual variability phytoplankton pigment concentration in the Peru and California Current systems. *Journal of Geophysical Research* 99, 7355–7370.
- Thorade, H., 1909. Über die Kalifornieschen Meeresströmungen, Oberflächentemperaturen und Strömungen and der Westüste Nordamerikas. *Annalen der Hydrographie und Maritimen Meteorologie* 17–34, 63–76.
- van Geen, A., Husby, C.M., 1996. Cadmium in the California Current system: tracer of past and present upwelling. *Journal of Geophysical Research* 101, 3489–3507.
- Wilkerson, F.P., Dugdale, R.C., 1987. The use of large shipboard barrels and drifters to study the effects of coastal upwelling on phytoplankton dynamics. *Limnology and Oceanography* 32, 368–382.